Dynamic Control of the Polarization of Intense Laser Beams via Optical Wave Mixing in Plasmas

P. Michel, L. Divol, D. Turnbull, and J. D. Moody
Lawrence Livermore National Laboratory, Livermore, California 94551, USA
(Received 18 July 2014; published 14 November 2014)

When intense laser beams overlap in plasmas, the refractive index modulation created by the beat wave via the ponderomotive force can lead to optical wave mixing phenomena similar to those used in crystals and photorefractive materials. A new comprehensive analytical description of the modification of the polarization state of laser beams crossing at arbitrary angles in a plasma is presented. It is shown that a laser-plasma system can be used to provide full control of the polarization state of a separate "probe" laser beam; simple analytical estimates and practical considerations are provided for the design of novel photonics devices such as laser-plasma polarizers and wave plates.

DOI: 10.1103/PhysRevLett.113.205001 PACS numbers: 52.25.Os, 42.25.Ja, 52.35.Mw, 52.38.−r

Optical wave mixing phenomena in plasmas have been extensively studied for more than forty years. Proposed applications have ranged from beat-wave particle acceleration [1,2] to plasma diagnostics [3,4] and laser pulse compression [5] or amplification [6]. More recently, novel techniques using plasmas have been proposed and demonstrated to control the propagation and properties of intense laser beams at intensities many orders of magnitude beyond the breaking point of "traditional" optics. For example, plasma mirrors have been successfully used to increase the contrast of intense laser pulses [7–10]. Plasma gratings are also now routinely used at the National Ignition Facility (NIF) [11] to dynamically deflect the flux of laser energy inside inertial confinement fusion (ICF) targets, in order to tune the implosion symmetry of the spherically imploded nuclear fuel [12,13] or to avoid regions most prone to backscatter losses inside the target [14,15]. Plasma gratings have also been used recently in ultraintense, ultrashort laser pulse experiments to diagnose the size of an x-ray source in the target plane [16].

In this Letter, we show that controlled optical wave mixing between a "probe" and a "pump" laser beam in a plasma can allow complete control of the polarization state of the probe beam. The probe's polarization can be adjusted by modifying the amplitude or the phase of its electric field; this is controlled by varying the pump intensity and tuning the phase velocity of the resulting beat wave via small wavelength shifts between the lasers. Using a Jones matrix analysis, we present an analytical description of the modification of the polarization for arbitrary crossing angles. These results are relevant to a wide variety of pump-probe laser-matter interaction experiments, as well as multi-laser-beam experiments for high energy density (HED) science or ICF on large scale laser facilities. We give simple analytical estimates and practical considerations for the design of novel photonics devices such as laser-plasma polarizers and wave plates.

The wave-mixing geometry is shown in Fig. 1. Two laser beams labelled 0 (the "pump") and 1 (the "probe") with arbitrary polarizations and with frequencies ω_0, ω_1 and wave vectors $\boldsymbol{k}_0, \boldsymbol{k}_1$ cross at an angle ψ; we define z as the bisector between $\boldsymbol{k}_0$, $\boldsymbol{k}_1$, and assume a copropagating geometry ($\psi < \pi/2$). We use the normalized vector potentials of the laser electric field, $\boldsymbol{a} = e\boldsymbol{A}/(m_e c^2)$, where the electric field is $\boldsymbol{E} = -\partial \boldsymbol{A}/(c\partial t) + \nabla\Phi$; in practical units, $a \simeq 8.55 \times 10^{-10}(I\lambda_\mu^2)^{1/2}$ where I is the laser intensity in W/cm^2 and λ_μ its wavelength in microns. For each beam $j(=0,1)$, we define the unit vectors $(\boldsymbol{p}_j, \boldsymbol{s}_j)$ in each plane of polarization such that $\boldsymbol{s}_j$ is perpendicular to the plane of incidence ($\boldsymbol{s}_0 = \boldsymbol{s}_1 \propto \boldsymbol{k}_0 \times \boldsymbol{k}_1$), and $\boldsymbol{p}_j$ is in the plane of incidence. The total electromagnetic potential is $\boldsymbol{a}(\boldsymbol{r}, t) = \mathrm{Re}[\boldsymbol{a}_0(z)e^{i\psi_0} + \boldsymbol{a}_1(z)e^{i\psi_1}]$, where $\psi_j = \boldsymbol{k}_j \cdot \boldsymbol{r} - \omega_j t$ and the envelopes $\boldsymbol{a}_0$, $\boldsymbol{a}_1$ are assumed to be at steady state and vary only along z. The plasma has an electron density n_e and frequency $\omega_{pe} = [4\pi n_e e^2/m_e]^{1/2}$ and refractive index $\eta_j = (1 - \omega_{pe}^2/\omega_j^2)^{1/2}$ (with $k_j = \eta_j \omega_j/c$).

As the two beams interact, the ponderomotive force of their beat wave drives a density (and, thus, refractive index) modulation in the plasma at the phase $\psi_b = \psi_0 - \psi_1 = k_b x - \omega_b t$, where $\boldsymbol{k}_b = \boldsymbol{k}_0 - \boldsymbol{k}_1$ and $\omega_b = \omega_0 - \omega_1$. We decompose the electron density into a background density (assumed constant in the following) and the modulation due to the beat wave: $n_e = n_0 + \mathrm{Re}[\delta n e^{i\psi_b}]$. The steady-state expression of the density modulation is $\delta n/n_0 = -\frac{1}{2}Kk_b^2 c^2 \omega_{p0}^{-2} \boldsymbol{a}_0 \cdot \boldsymbol{a}_1^*$ [17,18], where $\omega_{p0} = [4\pi n_0 e^2/m_e]^{1/2}$ and $K = \chi_e(1+\chi_i)/(1+\chi_e+\chi_i)$; the spatial variations of $|\delta n(z)|$ are assumed small compared to k_b^{-1} ($\sim\lambda_0$). The electron and ion ($\alpha = e, i$) susceptibilities at thermodynamic equilibrium are $\chi_\alpha = -\frac{1}{2}(k_b\lambda_{D\alpha})^{-2} Z'[v_b/(\sqrt{2}v_{T\alpha})]$, where Z is the plasma dispersion function, $v_b = \omega_b/k_b$ the beat wave phase velocity, $v_{T\alpha} = (T_\alpha/m_\alpha)^{1/2}$ the thermal velocity, T_α and m_α the temperature and mass, and $\lambda_{D\alpha} = v_{T\alpha}/\omega_{p\alpha}$ the Debye length.

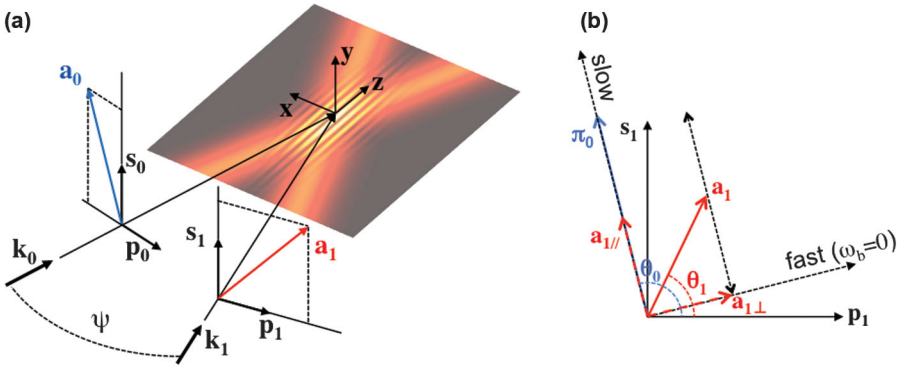

FIG. 1 (color). Interaction geometry between two laser beams (a "pump" and a "probe" with electric fields $\boldsymbol{a}_0$ and $\boldsymbol{a}_1$, respectively) in a plasma. (a) The beams cross at an angle ψ, forming a plasma grating via the ponderomotive force of the beat wave. (b) $\boldsymbol{\pi}_0$ is the projection of $\boldsymbol{a}_0$ in the plane of polarization of the probe beam. In the undepleted pump limit, the $\boldsymbol{a}_{1\perp}$ component of the probe perpendicular to $\boldsymbol{\pi}_0$ is unaffected by the coupling whereas the parallel component $\boldsymbol{a}_{1\|}$ has its amplitude or phase (or both) modified, depending on the phase velocity of the plasma grating (cf. Fig. 2).

Using Maxwell equations, the following one-dimensional coupled equations are derived for the vector envelopes:

$$2k_{1z}\boldsymbol{a}_1' = -i\frac{\omega_{p0}^2}{2c^2}\frac{\delta n^*}{n_0}\boldsymbol{a}_0, \tag{1}$$

$$2k_{0z}\boldsymbol{a}_0' = -i\frac{\omega_{p0}^2}{2c^2}\frac{\delta n}{n_0}\boldsymbol{a}_1, \tag{2}$$

where $k_{jz} = \boldsymbol{k}_j \cdot \boldsymbol{z}$, the prime denotes the derivative along z and the star represents the complex conjugate. These equations are similar to those used for coupled-mode theory for holography [19] and are valid for arbitrary crossing angles as long as the variations of the envelopes $\boldsymbol{a}_0, \boldsymbol{a}_1$ along the z direction are small compared to the laser wavelengths. Multiplying the equations by the unit vectors $(\boldsymbol{p}_1, \boldsymbol{s}_1)$ and $(\boldsymbol{p}_0, \boldsymbol{s}_0)$ allows us to rewrite these coupled equations in terms of the Jones vectors of the two waves in their $(\boldsymbol{p}_j, \boldsymbol{s}_j)$ polarization bases,

$$|a_j\rangle = \begin{pmatrix} a_{jp} \\ a_{js} \end{pmatrix};$$

in the following, the "bra" notation will denote the conjugate transpose (so that $\langle a_j|a_j\rangle = |a_j|^2$). The density perturbation can be expressed as $\delta n/n_0 = -\frac{1}{2}Kk_b^2c^2\omega_{p0}^{-2}\langle a_1|\pi_0\rangle$, where

$$|\pi_0\rangle = \begin{pmatrix} a_{0p}\cos(\psi) \\ a_{0s} \end{pmatrix}$$

is the projection of $\boldsymbol{a}_0$ onto the plane $(\boldsymbol{p}_1, \boldsymbol{s}_1)$ [cf. Fig. 1(b)]. If we further assume that the wavelengths of the two beams are close to each other, $\omega_0 \simeq \omega_1$, so that $k_1 \simeq k_0 = \eta_0\omega_0/c$, $k \simeq 2k_0\sin(\psi/2)$, and $k_{1z} \simeq k_{0z} = k_0\cos(\psi/2)$, then the coupled equations take the simple form

$$|a_1'\rangle = i\gamma^*\langle\pi_0|a_1\rangle|\pi_0\rangle, \tag{3}$$

$$|a_0'\rangle = i\gamma\langle\pi_1|a_0\rangle|\pi_1\rangle, \tag{4}$$

where z has been normalized by k_0. The coupling coefficient is $\gamma = \frac{1}{2}K\sin(\psi/2)\tan(\psi/2)$, and

$$|\pi_1\rangle = \begin{pmatrix} a_{1p}\cos(\psi) \\ a_{1s} \end{pmatrix}$$

is the projection of $\boldsymbol{a}_1$ onto $(\boldsymbol{p}_0, \boldsymbol{s}_0)$.

That system of equations describes the coupled evolutions of four complex field envelopes (the s and p components of each of the two laser beams) and are similar to the general case of two-wave mixing in photorefractive media [20–22]; here, unlike for some crystals, the initial isotropy of the plasma does not allow for cross coupling between the s and p components. Some conservation laws can be readily derived, e.g., $(|a_1|^2)' = -(|a_0|^2)' = 2\mathrm{Im}(\gamma)|\langle a_1|\pi_0\rangle|^2$ (total energy conservation), and $(a_{1p}^2 + a_{0p}^2)' = (a_{1s}^2 + a_{0s}^2)' = 0$ (i.e., energy conservation of the s and p components).

The system of Eqs. (3)–(4) does not have a closed solution for arbitrary crossing angles ψ, but much physical insight can be gained by assuming that the pump is unaffected by the interaction ($|a_0|^2 \gg |a_1|^2$). Equation (3) can be recast into $|a_1'\rangle = M_0|a_1\rangle$ where $M_0 = i\gamma^*|\pi_0\rangle\langle\pi_0|$ is a 2×2 matrix now assumed independent of z. The solution for $|a_1\rangle$ for an interaction from $z = 0$ to L is obtained by taking the exponential of M_0. The eigenvalues of M_0 are 0 and $i\gamma^*|\pi_0|^2$, and its eigenvectors are $|\pi_0\rangle$ and

$$|\rho_0\rangle = \begin{pmatrix} -a_{0s}^* \\ a_{0p}^*\cos(\psi) \end{pmatrix};$$

the eigenvectors are perpendicular, i.e., $\langle\pi_0|\rho_0\rangle = 0$. If we assume that the pump beam is linearly polarized and set (without loss of generality) the phase of a_0 to 0, the solution for the evolution of $|a_1\rangle$ then takes the simple form

$$|a_1(L)\rangle = R(-\theta_0)\begin{pmatrix} e^{i\gamma^*|\pi_0|^2k_0L} & 0 \\ 0 & 1 \end{pmatrix}R(\theta_0)|a_1(0)\rangle, \tag{5}$$

where θ_0 is the angle between $\boldsymbol{p}_1$ and $\boldsymbol{\pi}_0$ [cf. Fig. 1(b)] and

$$R(\theta_0) = \begin{pmatrix} \cos(\theta_0) & \sin(\theta_0) \\ -\sin(\theta_0) & \cos(\theta_0) \end{pmatrix}$$

is a rotation matrix by θ_0 in the plane $(\boldsymbol{p}_1, \boldsymbol{s}_1)$.

That expression makes the essential physics process of the wave mixing a lot more transparent: essentially, it shows that the interaction leaves the component $\boldsymbol{a}_{1\perp}$ of the probe perpendicular to $\boldsymbol{\pi}_0$ [cf. Fig. 1(b)] unchanged but multiplies the parallel component $\boldsymbol{a}_{1\parallel}$ by $\exp[i\gamma^*|\pi_0|^2 k_0 L]$. Practically, since $|\pi_0|^2 = |a_{0p}|^2\cos^2(\psi) + |a_{0s}|^2$, the coupling can be maximized by aligning the pump's electric field with the s direction, in which case $\pi_0 = a_0$. Whether the coupling affects the amplitude or phase of the probe beam (or both) depends on the plasma response term K, whose real and imaginary parts are plotted in Fig. 2.

Figure 2 was calculated for parameters typical of recent ICF or HED experiments, i.e., an electron density of 10% of critical (for a laser wavelength of 351 nm), an electron and ion temperature of 3 and 1 keV, respectively, and a crossing angle of 20 degrees in a helium plasma. The phase of $a_{1\parallel}$ is retarded with respect to $a_{1\perp}$ for $\mathrm{Re}(K) > 0$ (i.e., $|v_b| < c_s$, where $c_s = \sqrt{(ZT_e + 3T_i)/m_i}$ is the plasma sound speed) or accelerated for $\mathrm{Re}(K) < 0$ (i.e., for $|v_b| > c_s$ [23]), and the amplitude of $a_{1\parallel}$ exponentially grows for $\mathrm{Im}(K) > 0$ (i.e., $v_b > 0$) or decays for $\mathrm{Im}(K) < 0$ (i.e., $v_b < 0$).

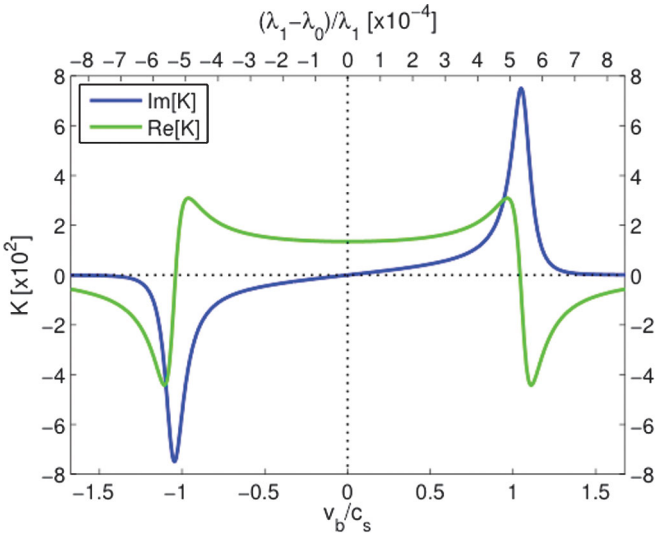

FIG. 2 (color). Plasma coupling coefficient K (defined in text) as a function of the phase velocity of the grating v_b normalized to the plasma sound speed c_s (lower x axis), or, equivalently, vs the frequency shift between the two laser beams (upper x axis), for the following parameters: $T_e = 3$ keV, $T_i = 1$ keV, $Z = 2$ (helium), $n_0 = 0.1 n_c$, and $\lambda_0 = 351$ nm. The phase of $a_{1\parallel}$ [cf. Fig. 1(b)] is retarded if $\mathrm{Re}(K) > 0$ [or accelerated if $\mathrm{Re}(K) < 0$], and its amplitude exponentially grows if $\mathrm{Im}(K) > 0$ [or decays if $\mathrm{Im}(K) < 0$].

We note two particularly interesting regimes for practical applications. The first corresponds to nondegenerate wave mixing with $v_b = \pm c_s$, where the beat wave has its phase velocity equal to the plasma sound speed and thus resonantly drives an ion-acoustic wave. Practically, this can be achieved by adjusting the frequency difference between the beams, as is now routinely done on the NIF to control energy transfer between laser beams entering ICF targets [24]. In this case, the plasma dielectric response $\epsilon = 1 + \chi_e + \chi_i$ vanishes, so the real part of K becomes 0, whereas its imaginary part reaches a maximum for $v_b = c_s$ (or minimum for $v_b = -c_s$; cf. Fig. 2).

In this case, the phase of a_1 remains constant, but its amplitude varies [the electric field vector evolves along the dashed line parallel to $\boldsymbol{\pi}_0$ in Fig. 1(b)]. This leads to a rotation of the polarization of a_1, from $\theta_1(0)$ to

$$\theta_1(L) = \theta_0 - \mathrm{atan}[e^{-\mathrm{Im}(\gamma)|\pi_0|^2 k_0 L} \tan[\theta_0 - \theta_1(0)]]. \quad (6)$$

For strong amplification $[\mathrm{Im}(\gamma)|\pi_0|^2 k_0 L \gg 1]$, we have $\theta_1(L) \simeq \theta_0$, i.e., the probe "aligns itself with the pump," whereas for strong decay $[-\mathrm{Im}(\gamma)|\pi_0|^2 k_0 L \gg 1]$, we get $\theta_1(L) \simeq \theta_0 - \pi/2$, i.e., the parallel component $a_{1\parallel}$ vanishes.

The case of a probe amplification ($v_b = c_s$) can be very efficient at rotating the polarization of the probe, albeit its amplitude will be affected as well. For example, for a pump linearly polarized along s with intensity 10^{15} W/cm^2 and for the same plasma parameters used in Fig. 2, we find that a probe originally polarized at $\theta_1 = 23°$ rotates by 45° over only 100 μm, though its power is also amplified by a factor ~6.

On the other hand, the case of strong probe decay with $v_b = -c_s$ ($\omega_1 = \omega_0 + k_b c_s$) presents a straightforward application as a "plasma polarizer" in the direction perpendicular to $\boldsymbol{\pi_0}$, as is conceptually represented in Fig. 3(a). The extinction ratio is then $\exp[-2\mathrm{Im}(\gamma)|\pi_0|^2 k_0 L]$. For example, using again the plasma conditions from Fig. 2 with an s polarized 10^{15} W/cm^2 pump, an extinction ratio of 10^{-5} can be achieved for an interaction length $L \simeq 300$ μm.

The second regime of interest is when the wave-mixing is degenerate ($\omega_0 = \omega_1$). In this case, the beat wave is a standing wave, and as is seen in Fig. 2, $\mathrm{Im}(K) = 0$, so $\gamma \in \mathrm{IR}$. This means that the amplitude of a_1 will remain unchanged (no energy transfer), but the phase of its $a_{1\parallel}$ component will be retarded. This corresponds to a birefringence of the "pump + plasma" system, and is consistent with recent work on ultrashort laser pulses propagation in gases by Wahlstrand *et al.* [25,26].

The axes perpendicular and parallel to $|\pi_0\rangle$ then, respectively, become the "fast" and "slow" axes [cf. Fig. 1(b)], with refraction indices

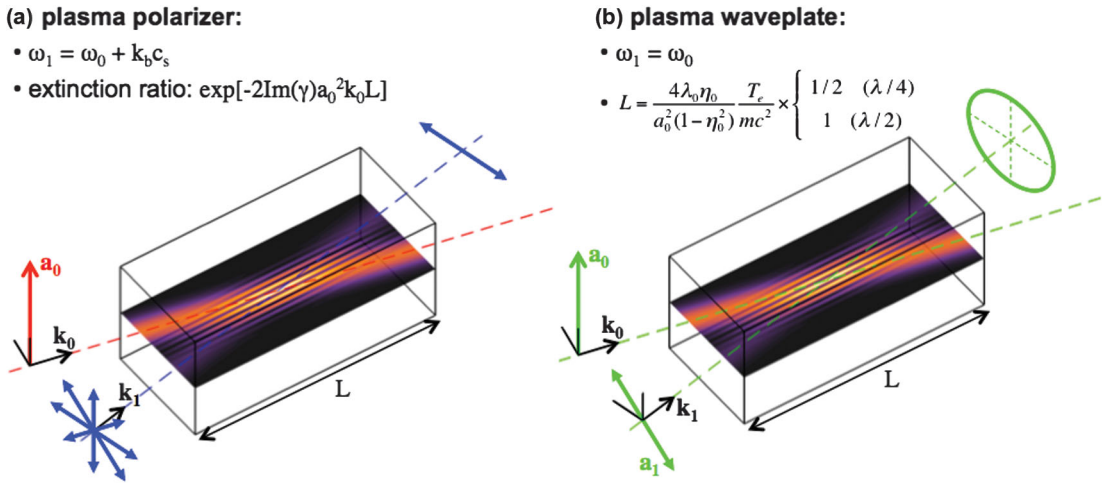

FIG. 3 (color). Conceptual design for: (a) a laser-plasma polarizer and (b) a laser-plasma wave plate.

$$\eta_{\mathrm{fast}} = \eta_0, \tag{7}$$

$$\eta_{\mathrm{slow}} = \eta_{\mathrm{fast}}\left(1 + \frac{K}{2}\sin^2(\psi/2)|\pi_0|^2\right). \tag{8}$$

When $\omega_0 = \omega_1$, the susceptibilities are simply $\chi_\alpha = (k_b\lambda_{D\alpha})^{-2}$ for $\alpha = e$ or i (electron or ion). If $\chi_i/\chi_e = ZT_e/T_i \gg 1$, K simplifies further to $K \simeq (k_b\lambda_{De})^{-2} = (1-\eta_0^2)/[4\eta_0^2\sin^2(\psi/2)T_e/(m_e c^2)]$.

This can be readily applied to the design of a "plasma wave plate," which is schematically represented in Fig. 3(b). From the expressions of the fast and slow refractive indices, the criteria on the interaction length L to design a quarter- or half-wave plate ("$\lambda/4$" or "$\lambda/2$") is

$$L = \frac{\lambda_0}{|\pi_0|^2\eta_0 K\sin^2(\psi/2)} \times \begin{cases} 1/2 & (\lambda/4) \\ 1 & (\lambda/2) \end{cases}, \tag{9}$$

$$\overset{ZT_e \gg T_i}{\simeq} \frac{4\eta_0\lambda_0}{|\pi_0|^2(1-\eta_0^2)}\frac{T_e}{m_e c^2} \times \begin{cases} 1/2 & (\lambda/4) \\ 1 & (\lambda/2) \end{cases}. \tag{10}$$

For the same plasma parameters used in Fig. 2 and the geometry from Fig. 3(b) (i.e., the pump is s polarized and the probe is initially linearly polarized at 45° from the plane of incidence), a pump intensity of 10^{15} W/cm^2 requires an interaction length of ~0.5 and 1 mm to achieve a quarter- and half-wave plate, respectively. For example, laser beams on the "inner cones" of the NIF have intensities of a few 10^{14} W/cm^2 but overlap over several millimeters, with initial linear polarizations rotated by 45° due to the azimuthal beam arrangement; therefore, these results show that, while propagating through ICF targets, the laser beams' polarizations are expected to acquire significant ellipticity.

Note that one can easily show that in the same undepleted pump regime, the formulae and the required interaction length remain the same for a counter-propagating geometry, i.e., by substituting ψ for $\pi - \psi$.

Achieving a circular polarization would, in principle, provide "polarization smoothing" of the probe laser beam, similar to those used at large scale laser facilities such as the NIF or the Omega laser at the Laboratory for Laser Energetics [27–29].

It is also worth noting that the behavior of the plasma grating is different for the degenerate vs nondegenerate cases. One can show from Eqs. (3)–(4) that $|\delta n|' = -f|\delta n|\mathrm{Im}(\gamma)$ and $\phi' = f\mathrm{Re}(\gamma)$, where ϕ is the phase of δn and $f = \langle\pi_1|\pi_1\rangle - \langle\pi_0|\pi_0\rangle$ is real. If $\omega_0 = \omega_1$ [$\mathrm{Im}(\gamma) = 0$], the amplitude of δn will be constant, but its phase will evolve along z. On the other hand, if $v_b = \pm c_s$ [$\mathrm{Re}(\gamma) = 0$], the amplitude of δn will vary, but its phase will stay constant and dephased from the beat wave's intensity pattern by $\pi/2$. These features are similar to what is observed in photorefractive media, except that the $\pi/2$ grating vs beat wave dephasing (allowing energy exchange between the beams) occurs for degenerate wave mixing in photorefractive crystals (vs nondegenerate in plasmas). For practical purposes, manipulating the polarization using the laser-induced plasma birefringence has the added advantage that as long as the amplitude of δn is small enough to prevent nonlinear effects (particle trapping, wave breaking, etc.), that amplitude will remain constant and presumably under control over the whole interaction length. Thus, in our previous numerical example of a 1 mm-long plasma half-wave plate (or 0.5 mm-long quarter-wave plate) with a pump intensity of 10^{15} W/cm^2 and a probe intensity of 10^{14} W/cm^2, the density perturbation level would remain very small, $|\delta n|/n_0 = 0.15\%$. It should also be noted that the experimental implementation of these concepts might reveal practical challenges due to the fact that the intensities required for the pump are typically high enough to trigger other laser-plasma mechanisms, such as collisional absorption, self-focusing, backscatter, etc.; assessing these secondary mechanisms will depend on the specific application and corresponding laser and plasma conditions.

In conclusion, we have shown that optical wave mixing in a plasma can allow a full control of the polarization state of laser beams. A Jones matrix analysis, valid for arbitrary crossing angles and initial polarization geometries, provides an intuitive physical picture of the effect of the wave mixing on the polarizations. Degenerate wave mixing ($\omega_0 = \omega_1$) can be used to control the dephasing between the probe components $a_{1\parallel}$ and $a_{1\perp}$ (parallel and perpendicular to the projection of the pump's electric field in the probe's plane of polarization), which allows the design of a laser-plasma wave plate. Nondegenerate wave mixing with $\omega_1 = \omega_0 \pm k_b c_s$ can be used to control the amplitude of $a_{1\parallel}$, allowing polarization rotation and the design of a laser-plasma polarizer. These systems constitute the basic building blocks for many active or passive optical systems such as ultrafast Pockel cells, etc. These results are relevant for a large variety of pump-probe or multi-laser-beam experiments and could lead to the development of new plasma-based photonics devices for the control of laser polarization at high intensity, with various possible applications such as dynamical polarization switching or optical beam smoothing.

This work was performed under the auspices of the U.S. Department of Energy by Lawrence Livermore National Laboratory under Contract No. DE-AC52-07NA27344.

[1] T. Tajima and J. M. Dawson, Phys. Rev. Lett. **43**, 267 (1979).
[2] C. E. Clayton, C. Joshi, C. Darrow, and D. Umstadter, Phys. Rev. Lett. **54**, 2343 (1985).
[3] N. M. Kroll, A. Ron, and N. Rostoker, Phys. Rev. Lett. **13**, 83 (1964).
[4] D. Froula, S. Glenzer, N. Luhmann, Jr., and J. Sheffield, *Plasma Scattering of Electromagnetic Radiation* (Academic, New York, 2011).
[5] V. M. Malkin, G. Shvets, and N. J. Fisch, Phys. Rev. Lett. **82**, 4448 (1999).
[6] G. Shvets, N. J. Fisch, A. Pukhov, and J. Meyer-ter-Vehn, Phys. Rev. Lett. **81**, 4879 (1998).
[7] C. Thaury, F. Quere, J. Geindre, A. Levy, T. Ceccotti, P. Monot, M. Bougeard, F. R. P. D'Oliveira, P. Audebert, R. Marjoribanks, and P. Martin, Nat. Phys. **3**, 424 (2007).
[8] G. Doumy, F. Quéré, O. Gobert, M. Perdrix, P. Martin, P. Audebert, J. C. Gauthier, J.-P. Geindre, and T. Wittmann, Phys. Rev. E **69**, 026402 (2004).
[9] B. Dromey, S. Kar, M. Zepf, and P. Foster, Rev. Sci. Instrum. **75**, 645 (2004).
[10] H. C. Kapteyn, A. Szoke, R. W. Falcone, and M. M. Murnane, Opt. Lett. **16**, 490 (1991).
[11] E. I. Moses, R. N. Boyd, B. A. Remington, C. J. Keane, and R. Al-Ayat, Phys. Plasmas **16**, 041006 (2009).
[12] P. Michel, L. Divol, E. A. Williams, S. Weber, C. A. Thomas, D. A. Callahan, S. W. Haan, J. D. Salmonson, S. Dixit, D. E. Hinkel, M. J. Edwards, B. J. MacGowan, J. D. Lindl, S. H. Glenzer, and L. J. Suter, Phys. Rev. Lett. **102**, 025004 (2009).
[13] S. H. Glenzer *et al.*, Science **327**, 1228 (2010).
[14] P. Michel *et al.*, Phys. Rev. E **83**, 046409 (2011).
[15] J. D. Moody *et al.*, Nat. Phys. **8**, 344 (2012).
[16] S. Monchocé, S. Kahaly, A. Leblanc, L. Videau, P. Combis, F. Réau, D. Garzella, P. D'Oliveira, P. Martin, and F. Quéré, Phys. Rev. Lett. **112**, 145008 (2014).
[17] E. A. Williams, B. I. Cohen, L. Divol, M. R. Dorr, J. A. Hittinger, D. E. Hinkel, A. B. Langdon, R. K. Kirkwood, D. H. Froula, and S. H. Glenzer, Phys. Plasmas **11**, 231 (2004).
[18] P. Michel, W. Rozmus, E. A. Williams, L. Divol, R. L. Berger, S. H. Glenzer, and D. A. Callahan, Phys. Plasmas **20**, 056308 (2013).
[19] H. Kogelnik, Bell Syst. Tech. J. **48**, 2909 (1969).
[20] A. Yariv and P. Yeh, *Optical Waves in Crystals: Propagation and Control of Laser Radiation*, Wiley Series in Pure and Applied Optics (Wiley, New York, 2002).
[21] P. Yeh, *Introduction to Photorefractive Nonlinear Optics*, Wiley Series in Pure and Applied Optics (Wiley, New York, 1993).
[22] P. Yeh, IEEE J. Quantum Electron. **25**, 484 (1989).
[23] Note, however, that $\mathrm{Re}[K]$ becomes positive again for larger values of $|v_b|$, not shown in this plot.
[24] P. Michel, L. Divol, E. A. Williams, C. A. Thomas, D. A. Callahan, S. Weber, S. W. Haan, J. D. Salmonson, N. B. Meezan, O. L. Landen, S. Dixit, D. E. Hinkel, M. J. Edwards, B. J. MacGowan, J. D. Lindl, S. H. Glenzer, and L. J. Suter, Phys. Plasmas **16**, 042702 (2009).
[25] J. K. Wahlstrand and H. M. Milchberg, Opt. Lett. **36**, 3822 (2011).
[26] J. K. Wahlstrand, J. H. Odhner, E. T. McCole, Y.-H. Cheng, J. P. Palastro, R. J. Levis, and H. M. Milchberg, Phys. Rev. A **87**, 053801 (2013).
[27] K. Tsubakimoto, M. Nakatsuka, H. Nakano, T. Kanabe, T. Jitsuno, and S. Nakai, Opt. Commun. **91**, 9 (1992).
[28] J. E. Rothenberg, Proc. SPIE Int. Soc. Opt. Eng. **2633**, 634 (1995).
[29] J. E. Rothenberg, Proc. SPIE Int. Soc. Opt. Eng. **3492**, 980 (1999).